Boundary-Layer Meteorology (2006) 118: 305–323
DOI 10.1007/s10546-005-2774-3

MODELLING THE ONE-DIMENSIONAL STABLE BOUNDARY LAYER WITH AN E–ℓ TURBULENCE CLOSURE SCHEME

WENSONG WENG* and PETER A. TAYLOR
Department of Earth and Space Science and Engineering, York University, 4700 Keele Street, North York, Ontario, Canada M3J 1P3

(Received in final form 03 February 2005)

Abstract. The atmospheric boundary layer (ABL) model of Weng and Taylor with E–ℓ turbulence closure is applied to simulate the one-dimensional stably stratified ABL. The model has been run for nine hours from specified initial wind, potential temperature and turbulent kinetic energy profiles, and with a specified cooling rate applied at the surface. Different runs are conducted for different cooling rates, geostrophic winds and surface roughnesses. The results are discussed and compared with other models, large-eddy simulations and published field data.

Keywords: Boundary-layer height, Inertial oscillation, Quasi-steady state, Stable boundary layer, Turbulence length scale.

1. Introduction

Much progress has been made in our understanding of the stably stratified atmospheric boundary layer (ABL) in the last twenty or thirty years. Numerical modelling, including large-eddy simulation (LES), has played an important role in the advance of our understanding.

In their LES study of the stable arctic ABL, Kosović and Curry (2000) used Beaufort Sea Arctic Stratus Experiment (BASE) data to impose initial and boundary conditions for simulating the horizontally homogeneous, clear-air Arctic boundary layer, characterized by a weak to moderate downward heat flux at the surface, and moderate to strong geostrophic winds. Brown et al. (1994) have also conducted a series of LES runs of the stable boundary layer (SBL) with a 'stochastic backscatter' subgrid model. Both showed a general agreement between the model results and observations or theoretical models.

Several commonly used 1.5-order turbulence closure schemes to model the ABL were discussed in Weng and Taylor (2003). In these closure schemes, the turbulent fluxes are locally related to mean vertical gradients and an eddy diffusivity, which depends on the turbulence kinetic energy, E, and a turbulent

* E-mail: wweng@yorku.ca

length scale, ℓ. The equation for the length scale can be either diagnostic or prognostic. The so-called E–ℓ closure scheme uses a prognostic equation for E and diagnostic equation for the turbulence length scale, while in an E–ϵ turbulence closure, prognostic equations for both E and the dissipation rate ϵ are used and the length scale is formulated from E and ϵ. This is effectively analogous to having a prognostic equation for ℓ. Previous applications of the standard ϵ equation in boundary-layer modelling studies yield too deep a boundary layer. Various investigators proposed modifications to the production and destruction terms in the ϵ equation, see for example, Detering and Etling (1985) and Xu and Taylor (1997) for the neutral ABL; Apsley and Castro (1997) and Weng and Taylor (2003) for the stable ABL. In their modelling study of the stably stratified boundary layer, Freedman and Jacobson (2003) also used a modified E–ϵ turbulent closure scheme through enforced consistency with Monin-Obukhov similarity theory. This leads to a dependence on the flux Richardson number, Ri_{f}, being included in either of the two usual coefficients, $c_{\epsilon 1}$ and $c_{\epsilon 2}$, in the ϵ equation (Ri_{f} was included in $c_{\epsilon 1}$ in their study).

Weng and Taylor (2003) have shown that the simple E–ℓ turbulence closure, which uses the turbulent kinetic energy equation together with a diagnostic equation for the turbulence length scale, performs quite well in most atmospheric conditions compared with the schemes that include the prognostic equations for both the turbulent kinetic energy and a length scale. In this paper, we further investigate the SBL using Weng and Taylor's ABL model with E–ℓ turbulence closure. A quasi-steady state of the stably stratified boundary layer is achieved by running the model for nine hours, and specifying a constant cooling rate at the surface. Different model runs are also made by exploring the parameter space by varying surface cooling rate, geostrophic wind and surface roughness. The model results are compared using hypotheses related to the stable ABL in a quasi-steady state. The bulk characteristics of the simulated quasi-steady, stably-stratified ABL are compared with other model studies and published observations.

2. The Model

For completeness, we briefly outline the ABL model of Weng and Taylor (2003) with an E–ℓ turbulence closure scheme. The model context is a one-dimensional (1D), horizontally homogeneous, dry boundary layer; its mean structure depends only on time t and the vertical coordinate z. It consists of three prognostic equations governing the evolution of the horizontal wind components U and V, and the potential temperature Θ:

$$\frac{\partial U}{\partial t} = f(V - V_{\mathrm{g}}) - \frac{\partial \langle uw \rangle}{\partial z}, \tag{1}$$

$$\frac{\partial V}{\partial t} = f(U_g - U) - \frac{\partial \langle vw \rangle}{\partial z}, \tag{2}$$

$$\frac{\partial \Theta}{\partial t} = -\frac{\partial \langle w\theta \rangle}{\partial z}. \tag{3}$$

Here u, v, w and θ are instantaneous fluctuations from the mean, f is the Coriolis parameter, U_g and V_g are components of the geostrophic wind, $-\langle uw \rangle$ and $-\langle vw \rangle$ are the (kinematic) shear stress components in the x and y directions respectively, $\langle w\theta \rangle$ is the vertical heat flux (positive upwards, in kinematic units) and angle brackets ($\langle\ \rangle$) represent an ensemble/short-time averaged mean. It is assumed that radiative flux divergence is small and can be neglected. The vertical flux terms are evaluated through an eddy diffusivity as

$$-\langle uw \rangle = K_m \frac{\partial U}{\partial z}, \tag{4}$$

$$-\langle vw \rangle = K_m \frac{\partial V}{\partial z}, \tag{5}$$

$$-\langle w\theta \rangle = K_h \frac{\partial \Theta}{\partial z}. \tag{6}$$

In the E–ℓ turbulence closure scheme, the eddy viscosity for momentum, K_m, and the eddy diffusivity for heat, K_h, are expressed as

$$K_m = \ell_m (\alpha E)^{1/2}, \tag{7}$$

$$K_h = \ell_m (\alpha E)^{1/2} \Big/ Pr, \tag{8}$$

where ℓ_m is a turbulent mixing length, the constant α is the ratio of the surface shear stress to the turbulent kinetic energy ($=0.3$ is used) and Pr is the turbulent Prandtl number (defined as $Pr = K_m/K_h$; the constant value of 0.85 is used here, see Kantha and Clayson, 2000). The usual 1D prognostic equation for E is

$$\frac{\partial E}{\partial t} = -\langle uw \rangle \frac{\partial U}{\partial z} - \langle vw \rangle \frac{\partial V}{\partial z} + \beta g \langle w\theta \rangle - \epsilon + \frac{\partial}{\partial z}\left(K_e \frac{\partial E}{\partial z} \right), \tag{9}$$

where β is the coefficient of thermal expansion and g is the acceleration due to gravity. The vertical diffusion coefficient, K_e, is assumed equal to K_m. The first two terms on the R.H.S. of Equation (9) represent turbulent kinetic energy production by the shear, the third is the buoyancy term, the fourth is the dissipation and the last term represents the diffusion of E in the vertical. The dissipation rate of turbulence kinetic energy, ϵ, is expressed as

$$\epsilon = \frac{(\alpha E)^{3/2}}{\ell_d}, \tag{10}$$

where ℓ_d is a dissipation length scale.

In the E–ℓ closure scheme, following Delage (1974) for stable flow, the turbulent length scales are modelled as follows:

$$\frac{1}{\ell_m} = \frac{1}{\kappa(z+z_0)} + \frac{1}{\ell_0} + \frac{\beta_c}{\kappa L_o}, \tag{11}$$

$$\frac{1}{\ell_d} = \frac{1}{\kappa(z+z_0)} + \frac{1}{\ell_0} + \frac{(\beta_c - 1)}{\kappa L_o}, \tag{12}$$

where the von Kármán constant $\kappa = 0.4$, z_0 is the surface roughness length, β_c is an empirical constant ($=4.8$) and L_o is the local Obukhov length, dependent on z and t, and defined by

$$L_o = -\frac{\left(\langle uw\rangle^2 + \langle vw\rangle^2\right)^{3/4}}{\kappa\beta g\langle w\theta\rangle}. \tag{13}$$

Here, ℓ_0 is a limiting length scale to the eddies under neutral thermal stratification, and may be set either as a constant (Mason and King, 1984) or may be related to the geostrophic wind speed and Coriolis parameter, $\ell_0 = 0.00027|\mathbf{U_g}|f^{-1}$ (Weng and Taylor, 2003). Here, we set ℓ_0 as a constant, which is taken to be 40 m.

Equation (12) is deduced from Equation (9) with the assumption of a constant flux layer. We note that from the length-scale formulae (11) and (12), ℓ_m and ℓ_d are proportional to $z + z_0$ near the ground and limited by ℓ_0 and $\kappa\beta_c^{-1}L_O$ higher up. As the boundary layer becomes more stable, the effects of the thermal term (involving L_O) will dominate and the value of ℓ_d is larger than that of ℓ_m.

The model uses a stretched vertical coordinate (a log-linear transform) to ensure sufficient resolution near the surface and to resolve strong vertical gradients. Equations are transformed into the new coordinate system before they are discretized into their finite difference equivalents. Flow variables are stored on a staggered grid, where mean variables (U, V and T) are at layer

midpoints and turbulent quantities (E and turbulent fluxes) are at the lower boundary level ($z=0$) and z_t (the top of the computation domain, set to 4000 m). To obtain a smooth solution, especially in the top part of the boundary layer, 301 grid points and a time step of 10 s are used. The numerical scheme employed for time integration is Crank-Nicolson. The resulting set of difference equations is solved using a block **LU** factorization algorithm (Karpik, 1988).

The surface boundary conditions used are a non-slip condition for velocity ($U=V=0$), a specified cooling rate for potential temperature (Θ) and the assumption that production balances the dissipation of the turbulent kinetic energy ($P=\epsilon$). At the upper boundary, we specify $(U, V)=(U_g, V_g)$, $\Theta=\Theta_g$ (constant) and set the vertical derivatives of E, ϵ, shear stresses and other turbulent fluxes to zero.

3. Results and Discussions

The model is used to study a simple, shear-driven, stable boundary layer. Unlike in Weng and Taylor (2003) where the simulations started from a neutral stratification wind profile, here simulations start from constant $|\mathbf{U_g}|$ to avoid substantial inertial oscillations above the stable boundary layer. The model is run for nine hours following a 'transition' from neutral stratification near the surface to a stable situation with a specified cooling rate at the surface.

A total of 50 simulations were conducted. The common parameters used in all the runs are the Coriolis parameter, $f=1.39\times10^{-4}$ s^{-1} and the reference potential temperature, $\Theta_0=263.5$ K. The initial conditions for wind, potential temperature and E profiles are as follows, $(U, V)=(U_g, V_g)$ for $z > 0$ m; $\Theta=265$ K for $0\le z\le 100$ m and, in most cases, increasing at 0.01 K m^{-1} to the domain top; $E=0.4(1-z/250)^3$ m^2 s^{-2} for $0\le z\le 250$ m and a minimum value of 10^{-9} m^2 s^{-2} for the rest of the grid points. Other quantities are initialized as follows: $\langle uw\rangle=0.3E$, $\langle vw\rangle=\langle w\theta\rangle=0$; ℓ_m and ℓ_d from Equations (11) and (12) for neutral flow and K_m, K_h and ϵ from Equations (7)–(8) and (10) respectively. All the other parameters and a summary of forty-two of the runs can be found in Table I. To study the effects of the initial potential temperature inversion strength on the SBL, eight further runs are carried out. The parameters used in the seven Runs G1–G7 are the same as those corresponding ones in Run A1–Run A7 except that the initial potential temperature $\Theta(z)=$ constant is used for all heights. The parameters used in Run H2 are the same as Run A2 except that the strength of the initial potential temperature inversion is 0.005 K m^{-1} instead of 0.01 K m^{-1}. Note that Run A2 corresponds to the GEWEX (Global Energy and Water Cycle Experiment) Atmospheric Boundary Layer Study – GABLS case, which is used in

TABLE I
Some parameters used in the simulations of the SBL.

Runs	Cooling rate (K h^{-1})	(U_g, V_g) (m s^{-1})	z_0 (m)
A			
1	0.125	(8,0)	0.1
2	0.25	(8,0)	0.1
3	0.5	(8,0)	0.1
4	1.0	(8,0)	0.1
5	1.5	(8,0)	0.1
6	2.0	(8,0)	0.1
7	2.5	(8,0)	0.1
B			
1	0.125	(8,0)	0.01
2	0.25	(8,0)	0.01
3	0.5	(8,0)	0.01
4	1.0	(8,0)	0.01
5	1.5	(8,0)	0.01
6	2.0	(8,0)	0.01
7	2.5	(8,0)	0.01
C			
1	0.125	(10,0)	0.1
2	0.25	(10,0)	0.1
3	0.5	(10,0)	0.1
4	1.0	(10,0)	0.1
5	1.5	(10,0)	0.1
6	2.0	(10,0)	0.1
7	2.5	(10,0)	0.1
D			
1	0.125	(10,0)	0.01
2	0.25	(10,0)	0.01
3	0.5	(10,0)	0.01
4	1.0	(10,0)	0.01
5	1.5	(10,0)	0.01
6	2.0	(10,0)	0.01
7	2.5	(10,0)	0.01
E			
1	0.125	(5,0)	0.1
2	0.25	(5,0)	0.1
3	0.5	(5,0)	0.1
4	1.0	(5,0)	0.1

Table I. Continued.

Runs	Cooling rate (K h^{-1})	(U_g, V_g) (m s^{-1})	z_0 (m)
5	1.5	(5,0)	0.1
6	2.0	(5,0)	0.1
7	2.5	(5,0)	0.1
F			
1	0.125	(5,0)	0.01
2	0.25	(5,0)	0.01
3	0.5	(5,0)	0.01
4	1.0	(5,0)	0.01
5	1.5	(5,0)	0.01
6	2.0	(5,0)	0.01
7	2.5	(5,0)	0.01

the single-column model intercomparison, see Cuxart et al. (2005). We first look at this GABLS case.

A sensitivity study was carried out to test our set-up with a smaller integration time step ($dt = 5$ s) and a finer grid size ($N_t = 601$) and the effect of the capped temperature inversion strength. Figure 1 shows the time evolution of the surface values of u_{*0}, $\langle w\theta \rangle_0$, L_O, and h_τ (see below for the definition) from Run A2 with two different time steps and grid sizes, and from Runs G2 and H2. The results from the two A2 runs are almost identical for those surface values, at least for the first nine hours after transition. However, there are some oscillations and differences in h_τ for the first few hours. The noise is much reduced for the higher resolution and the discrepancies almost disappear in the last four or five hours. The results presented in the remainder of the paper are all from runs with $dt = 10$ s and $N_t = 301$ unless stated otherwise.

The effects of the capped temperature inversions are mainly on h_τ, especially for the first three hours after transition. After four hours, h_τ is almost a constant. There is little effect of the capped temperature inversions on surface values of u_*, $\langle w\theta \rangle$ and L_O. If we are mainly interested in the quasi-steady model results, the capped temperature inversions produce slightly smaller values of h_τ. There are almost no differences for the surface values of u_*, $\langle w\theta \rangle$ and L_O, see also Figure 7.

Figure 2 shows the model predicted vertical profiles of the wind speed ($\sqrt{U^2 + V^2}$), potential temperature (Θ), shear stress (τ) and heat flux ($\langle w\theta \rangle$) at different times after the transition, for Run A2. The development of the stable boundary layer appears reasonable – a supergeostrophic wind or nocturnal jet is apparent at low levels and the convex shape of the Θ profile is

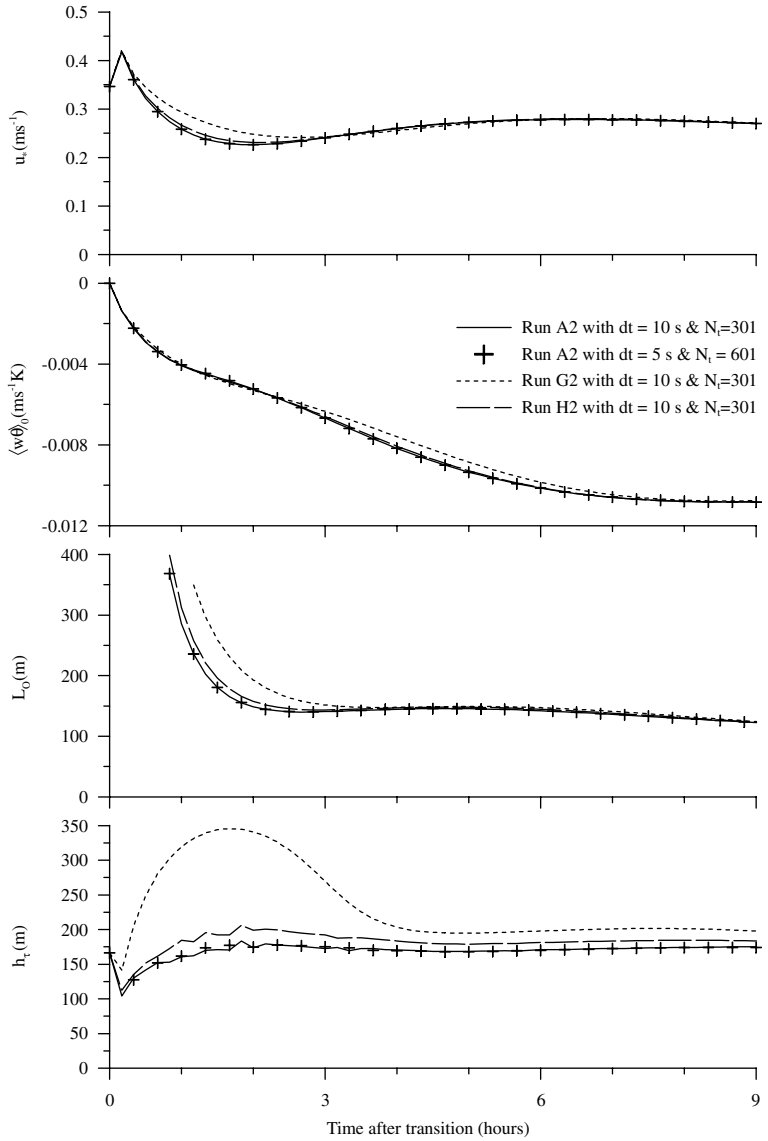

Figure 1. Time evolution of the surface friction velocity (u_{*0}), heat flux ($\langle w\theta\rangle_0$), surface Obukhov length (L_O) and boundary-layer height (h_τ) with different time steps and grid sizes from Run A2, G2 and H2.

consistent with expectations for a turbulence-driven SBL (André and Mahrt, 1982).

Due to the net loss of heat to the ground and no compensating heat flux at the top, the boundary layer as a whole must cool. A quasi-steady state or stationary stable boundary layer is achieved if the turbulent fluxes are

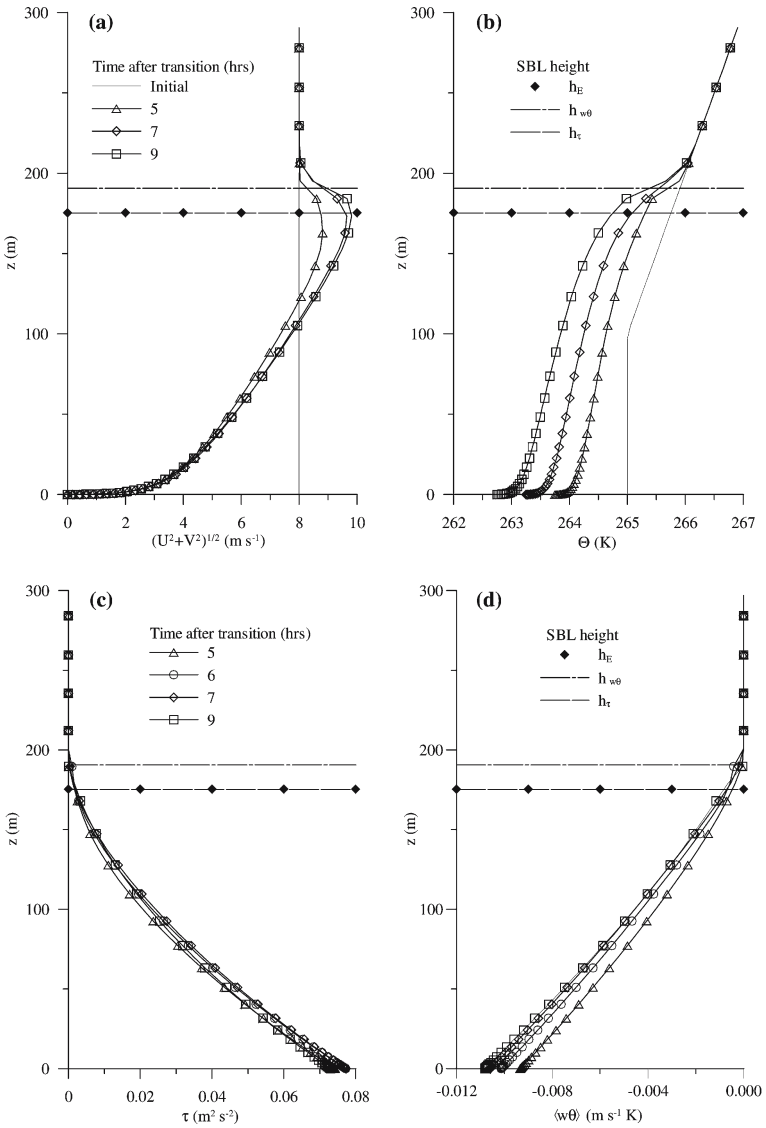

Figure 2. Vertical profiles of mean (a) wind speed, (b) potential temperature (c) shear stress and (d) heat flux at three different times during the cooling period from Run A2. Calculated boundary-layer heights at the ninth hours are also shown. Open symbols correspond to every second grid level.

independent of time (Nieuwstadt, 1984). Although the vertical profile of τ does not change much after five hours cooling, the vertical profile of $\langle w\theta \rangle$ continues to change for two more hours. We can say that after seven hours cooling, the stable boundary layer reaches its quasi-steady or stationary state, see Figure 2c and 2d.

One of the important parameters for ABL modelling is the depth of the boundary layer, h. The most commonly used definition is that h is the height where a turbulent quantity falls to 5% of its surface value. This turbulent quantity can be turbulent kinetic energy, E (Weng and Taylor, 2003) or heat flux, $\langle w\theta \rangle$ (Brown et al., 1994; Freedman and Jacobson, 2003) or shear stress, τ (Kantha and Clayson, 2000; Cuxart et al., 2005). These heights are here denoted as h_E, $h_{\langle w\theta \rangle}$ and h_τ respectively. Based on the ninth-hour model results, calculated boundary-layer heights h_E, $h_{\langle w\theta \rangle}$ and h_τ are also shown in Figure 2. The value of h_E is almost identical as that of h_τ and both are smaller than that of $h_{\langle w\theta \rangle}$ (this is true for all our model runs). Similar results were found in other models, see Cuxart et al. (2005). We can see that the maximum wind speed occurs at h_τ and above $h_{\langle w\theta \rangle}$ the turbulence almost diminishes.

For the quasi-steady state SBL, Zilitinkevich (1972) suggested that the boundary-layer height can be estimated from

$$h = c(u_* L_O/f)^{1/2}, \tag{14}$$

where c is a constant and L_o here is the surface value. From his local scaling model, Nieuwstadt (1985) found that $c^2 = \sqrt{3}\kappa Ri_f$, where Ri_f is the flux Richardson number. Freedman and Jacobson (2003) showed that $Ri_f \to 1/\beta_c$ from Monin-Obukhov similarity theory. Taking the value used here, $\beta_c = 4.8$, we have $Ri_f \approx 0.21$. which leads to $c \approx 0.38$, slightly smaller than the value $c \approx 0.4$ given by Garratt (1982). From our model results at the ninth hour, $u_* = 0.27$ m s^{-1} and $L_O = 122.5$ m, Equation (14) predicts $h = 185$ m with $c = 0.38$. This compares well with our model results of (h_E, $h_{\langle w\theta \rangle}$, h_τ) = (175,191,175) m.

For a stationary SBL, Nieuwstadt (1984) suggested

$$\tau/u_{*0}^2 = (1 - z/h)^{3/2}, \tag{15}$$

$$\langle w\theta \rangle / \langle w\theta \rangle_0 = (1 - z/h), \tag{16}$$

where the subscript '0' represents the surface value. Our model results, together with the theoretical prediction of Nieuwstadt, are shown in Figure 3. The agreement is very good except close to the top of the boundary layer. Although Equations (15) and (16) are deduced for the stationary SBL and we note that for Run A2, the stable boundary layer reaches its quasi-steady state only after seven hours of cooling, the fifth hour's data can also be well described by these similarity equations. This implies that our model results obey the similarity form before the boundary layer fully achieves a quasi-steady state.

From his stationary SBL model, Nieuwstadt (1985) has also shown that the normalized eddy viscosity can be expressed as

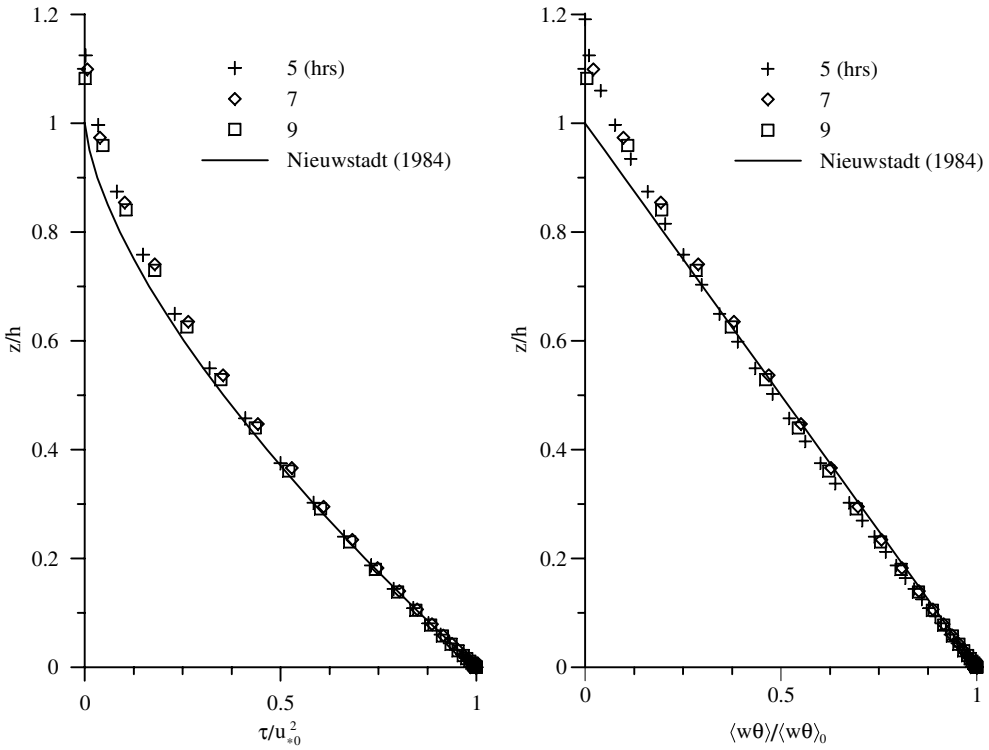

Figure 3. Turbulent fluxes from Run A2, normalized by their surface values as a function of non-dimensional height (z/h), are compared with Nieuwstadt's theoretical predictions. $h = h_\tau$ for model results.

$$\frac{K_m}{u_* L_o} = \frac{\kappa z/L_o (1 - z/h)^2}{1 + \beta_c z/L_o}. \tag{17}$$

Here L_o is a surface value. Our model results, together with the theoretical profiles, are shown in Figure 4, where it can be seen that the agreement is quite good except in the top part of the boundary layer. Similar results were also found in Freedman and Jacobson's (2003) study, who used a E–ϵ turbulence closure with a modified ϵ equation, see their Figure 7.

Although we might regard the SBL as reaching its quasi-steady state after seven hours of constant cooling, it is interesting to see how steady the SBL really is. For Case A2, we have run the model for a total of 126 hours, which is about 10 times the period of an inertial oscillation, $\mathscr{T}$ ($= 2\pi/f \approx 12.556$ h). Figure 5 shows wind speeds and wind hodographs at three different heights. For the first couple of $\mathscr{T}$ after the transition, there are quite large changes in wind speed, especially around the boundary-layer height. The wind speed levels off thereafter for the lower part of boundary layer (see wind speeds at

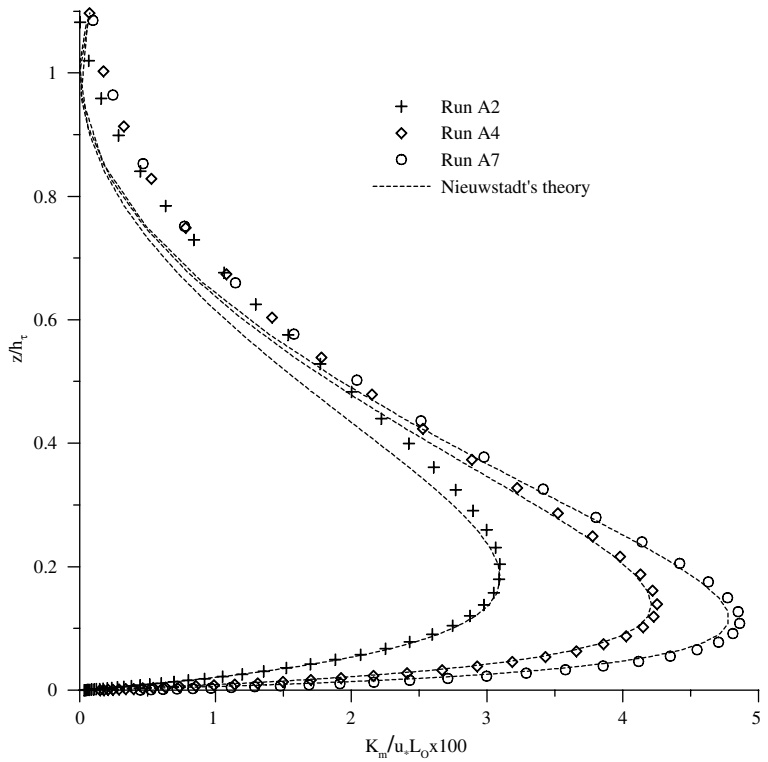

Figure 4. Vertical profiles of non-dimensional eddy viscosity, K_m vs. z/h_τ from Runs A, compared with Nieuwstadt's theory (1985).

$z = 10,\ 100$ m), while the wind speed at $z = 175$ m (the height where the boundary-layer height, h_τ, is calculated from the definition at the ninth hour) oscillates with an amplitude that reduces slowly. At the time of 10 $\mathscr{T}$, the amplitude is about 0.2 m s^{-1}. From the wind hodograph plot, one can see that wind direction changes little for the lower part of the boundary layer a few hours after transition. For the wind speed at $z = 175$ m, the effect of an inertial oscillation can also be clearly seen.

Figure 6 shows the time evolution of the surface friction velocity (u_{*0}), the surface heat flux ($\langle w\theta \rangle_0$), the surface Obukhov length (L_o) and the boundary-layer height (h_τ) from runs in group A. An initial increase in u_{*0} for a very short period of time is due to the fact that the model adjusts itself after using the specified initial profile. If the model is run from its neutral boundary-layer state with a specified cooling rate, u_{*0} decreases immediately, see Weng and Taylor (2003). There are fairly rapid decreases of u_{*0} within the first two hours after the transition, which then level off, while decreases of $\langle w\theta \rangle_0$ take longer, especially for the relative large cooling rates. Note also there are local maxima in $\langle w\theta \rangle_0$ for the large cooling rates, and the Obukhov length and the

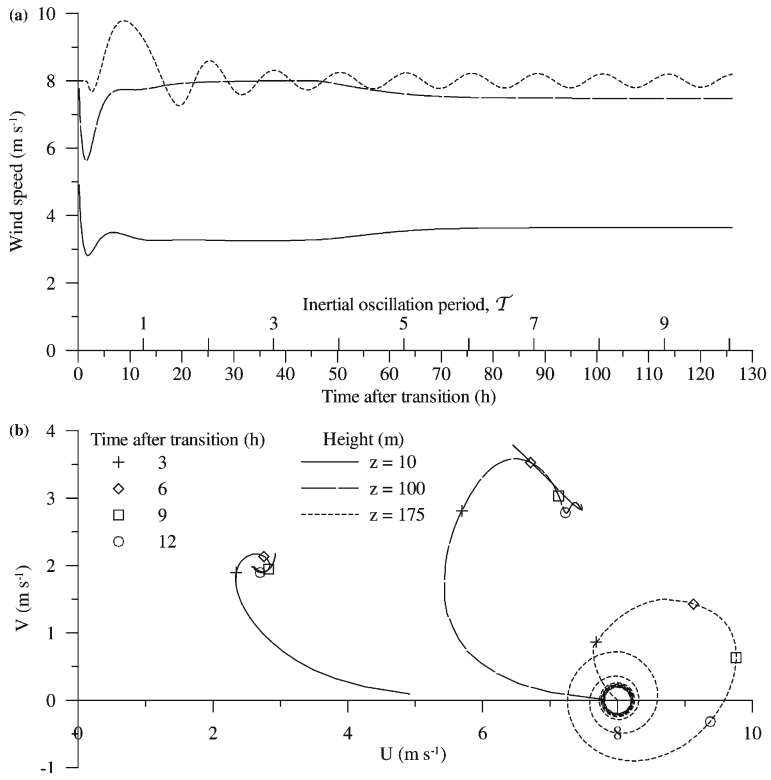

Figure 5. (a) evolution of the wind speed with time, and (b) wind hodographs at three different heights from Run A2.

boundary-layer height level off very quickly after the initial quick variation, despite continuous changes of u_{*0} and $\langle w\theta\rangle_0$. Small oscillations are found in h_τ for the first few hours, especially for the lower cooling rates. Note from Figure 1 that these oscillations are reduced in computations with higher vertical resolution. Some of the useful parameters for runs in group A at the ninth hour are listed in Table II. As expected, the boundary-layer depth, h_τ, the turbulent kinetic energy, E, the friction velocity, u_{*0}, and the Obukhov length, L_o decrease as the stability increases, while the downward heat flux, $-\langle w\theta\rangle_0$ and the surface mean wind angle or the surface stress angle, α, increase as the stability increases.

The model has simulated very simple, horizontally homogenous SBL situations and it is difficult to make detailed comparisons with field observations. Here, we look at several bulk parameters compared with published field data and with other modelling results.

Model predictions of the Zilitinkevich constant, $c = h(f/u_* L_o)^{1/2}$, the geostrophic drag coefficient, $C_g = \left(u_*/|\mathbf{U_g}|\right)^2$, and the surface mean wind

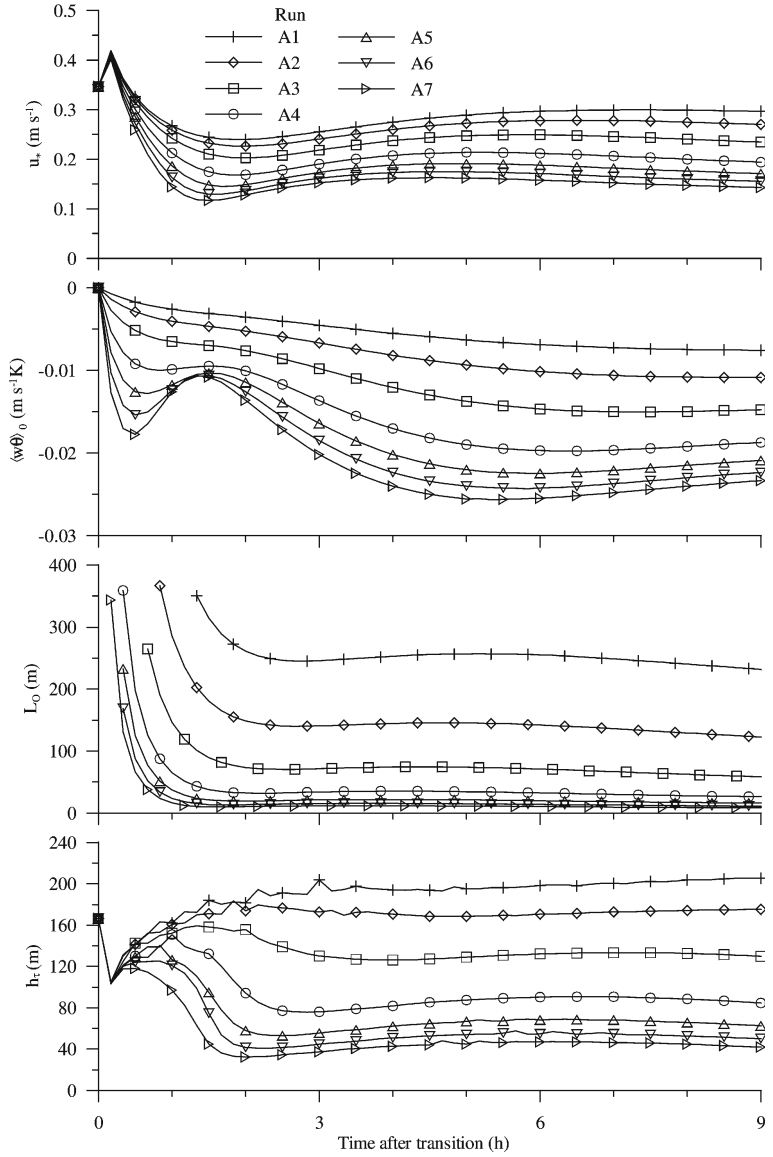

Figure 6. Evolution of the surface friction velocity (u_{*0}), heat flux ($\langle w\theta \rangle_0$), surface Obukhov length (L_O) and boundary-layer height (h_τ) under different cooling rate from Runs A.

angle, α, plotted against the stability parameter, $\mu = \kappa\, u_*/fL_o$, are shown in Figure 7. These plots are the results after nine hours and include data from all sets of runs (A–F) listed in Table I and from Runs G. Also shown are the modified $E-\epsilon$ turbulence closure model results of Freedman and Jacobson (2003), some LES results of Kosovic and Curry (2000) and Brown et al.

TABLE II

Final values (after nine hours) of some characteristics of simulated SBL for runs in group A ($|\mathbf{U_g}| = 8$ m s^{-1} and $z_0 = 0.1$ m).

Run	E_0 (m^2 s^{-2})	u_{*0} (m s^{-1})	$\langle w\theta\rangle_0$ (m s^{-1} K)	h_τ (m)	L_O (m)	α (degree)
A1	0.293	0.297	−0.0076	227.8	231.9	33.7
A2	0.244	0.270	−0.0108	175.2	122.5	35.7
A3	0.183	0.234	−0.0148	129.7	58.6	39.1
A4	0.126	0.194	−0.0187	84.4	26.3	43.5
A5	0.098	0.171	−0.0209	62.5	16.1	46.0
A6	0.080	0.155	−0.0224	49.9	11.3	47.7
A7	0.068	0.143	−0.0233	41.9	8.4	48.8

(1994), and field data of Caughey et al. (1979) and Lenschow et al. (1988). The scatter in LES (probably due to the different subgrid parameterizations and domain sizes used) and field data (possible effects of temporal variability, slope effects and spatial heterogeneity) makes it difficulty to establish the model's accuracy. The broad tendency is that c and α increase with stability, while C_g decreases with stability, as found in our model prediction and in the observations.

There is not much difference in model results of Runs A and G except in near-neutral conditions (small values of μ). The capped temperature inversion layer appears to exert little effect on these parameters for a quasi-steady SBL.

In our model, the effects of the geostrophic wind speed, $|\mathbf{U_g}|$, and the surface roughness length, z_0, on c are small. Most of the differences are confined to $\mu < 15$, corresponding to near-neutral conditions. The value of c first increases as μ increases, from around 0.2 for $\mu \approx 0$ to 0.4 at $\mu \approx 10$ and then levels off as μ increase further. For $\mu > 20$, it is almost a constant and $c \approx 0.45$. Our E–ℓ model results for c are slightly larger than those of the modified E–ϵ model by Freedman and Jacobson (2003). The LES results of Brown et al. (1994) and the field data of Caughey et al. (1979) indicate that c is larger, but the data of Kantha and Clayson (2000) and Lenschow et al. (1988) are compatible with our model results. According to theoretical modelling studies, the relatively high value of Caughey et al. (1979) is apparently appropriate to the early stages of development of the stable layer but c progressively decreases as a steady state is approached, see Pasquill and Smith (1983).

Our model results show good agreement with those of Freedman and Jacobson, who used an E–ϵ turbulence closure with a modified ϵ equation

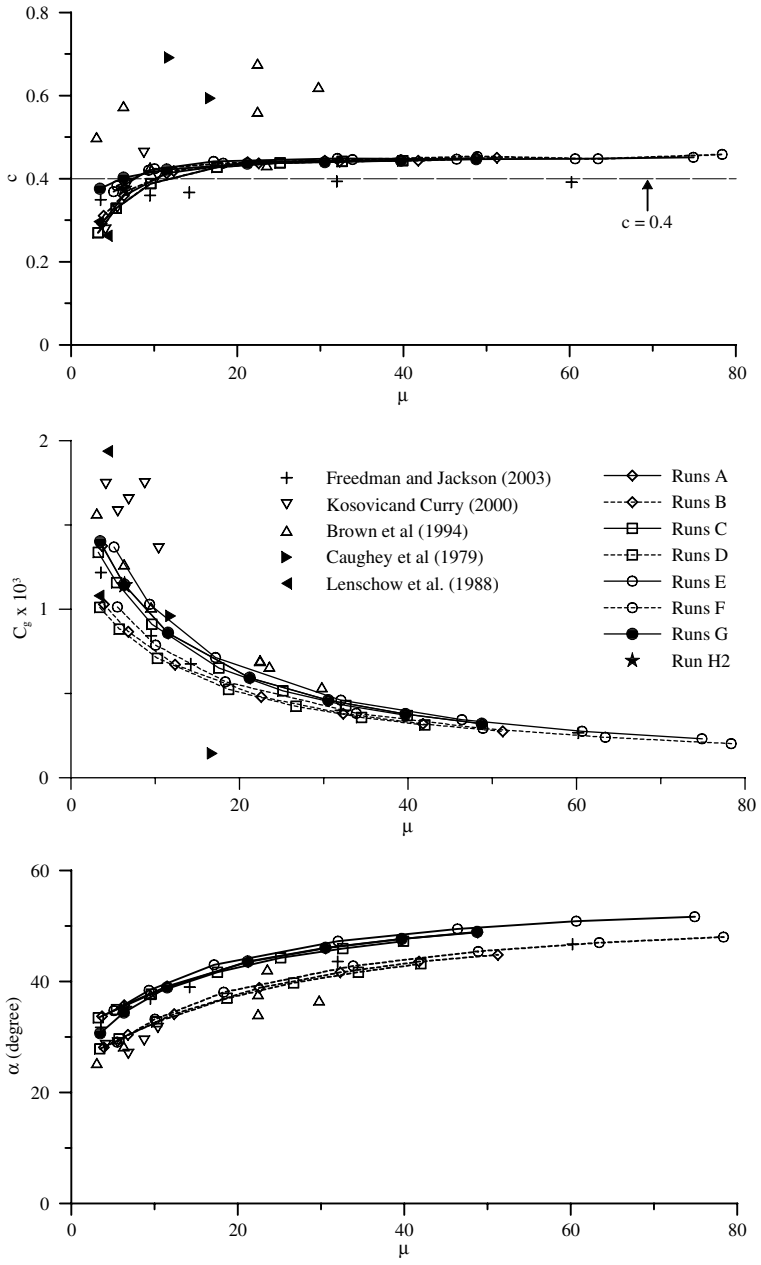

Figure 7. Variations of the Zilitinkevich constant (c), the geostrophic drag coefficient (C_g) and surface mean wind angle (α) with the stability μ ($=\kappa\, u_*/fL_o$). Each set of runs (A–G) has fixed values of (U_g,V_g) and z_0 but varying cooling rate leading to a range of μ values. For Run H2, $\mu \approx 6.3$.

through enforced consistency with Monin-Obukhov similarity theory. There is little effect of U_g on C_g and α. However, the effect of z_0 on C_g and α is more pronounced; see Figure 7 and compare Runs A and B for example. For small values of μ, there are differences in C_g, and the larger the value of surface roughness, the larger is C_g. As stability increases, the difference becomes small. At $\mu = 40$, it almost disappears. For a given stability, large values of the surface roughness cause a large surface wind angle. The two groups of curves corresponds to two different surface roughness. The difference in α with two different z_0 values remains almost the same for all stabilities in our runs.

4. Summary and Conclusions

A series of stable atmospheric boundary layers have been simulated with the ABL model of Weng and Taylor (2003). The stable boundary layer was developed by applying surface cooling to a specified initial state. Different values of cooling rate, geostrophic wind and surface roughness are also used in the simulations. The model results show good agreement with Nieuwstadt's (1985) theory, the modified E–ϵ model results of Freedman and Jacobson (2003), and, to a lesser extent, with the LES model results of Brown et al. (1994) and Kosović and Curry (2000) and with the field data of Caughey et al. (1979) and Lenschow et al. (1988)

Some effects of inertial oscillations are noted in the boundary layer and just above. The effect of an elevated capped temperature inversion is more pronounced on h_τ than on surface values of u_*, $\langle w\theta \rangle$ and L_O, especially for near-neutral conditions. Zilitinkevich's 'constant', c, is not really a constant, especially for low stability, $\mu < 10$. The present model results show that c increases quite rapidly, from around 0.2 for $\mu \approx 0$ to 0.4 for $\mu \approx 10$, and then levels off to about 0.45 as μ increases. This value is slightly higher than 0.4 suggested by Garratt (1982), but is in the range of 0.2 to 0.7 quoted by Pasquill and Smith (1983) from various empirical estimates. There is very little effect of the geostrophic wind on c, the drag coefficient, C_g and surface mean wind angle, α, when these quantities are plotted against the stability parameter, $\mu = \kappa\, u_*/fL_o$. The surface roughness (z_0) also exerts little effect on c while the effects of z_0 on C_g are mostly for $\mu < 30$ and the effect almost disappears for $\mu > 40$. However, the effect of z_0 on α remains almost the same across the stability range of our model runs, at about 4 to 5 degrees between $z_0 = 0.01$ and 0.1 m.

Our present modelling studies of the stable boundary layer are for simple situations, i.e., by applying a surface cooling rate. Future work will incorporate a soil model or land surface scheme coupled to the surface energy budget.

Acknowledgements

The authors thank Dr. Freedman for providing some of the data used in this paper. This research has been funded by grants from the Natural Science and Engineering Research Council of Canada.

References

André, J. C. and Mahrt, L.: 1982, 'The Nocturnal Surface Inversion and Influence of Clear-Air Radiative Cooling', *J. Atmos. Sci.* **39**, 864–878.

Apsley, D. D. and Castro, I. P.: 1997, 'A Limited-Length Scale K–ϵ Model for the Neutral and Stably-Stratified Atmospheric Boundary Layer', *Boundary-Layer Meteorol.* **83**, 75–98.

Brown, A. R., Derbyshire, S. H. and Mason, P. J.: 1994, 'Large-Eddy Simulation of Stable Atmospheric Boundary Layers with a Revised Stochastic Subgrid Model', *Quart. J. Roy. Meteorol. Soc.* **120**, 1485–1512.

Caughey, S. J., Wyngaard, J. C. and Kaimal, J. C.: 1979, 'Turbulence in the Evolving Stable Boundary Layer', *J. Atmos. Sci.* **36**, 1041–1052.

Cuxart, J., Holtslag, A. A. M., Bazile, E., Beare. R. J., Beljaars, A., Cheng, A., Conangle, L., Ek, M., Fredman, F. Ramdi, R., Kerstein, A., Kitagawa, H., Lenderink, G., Lewellen, D., Mailhot, J., Mauritsen, T., Perov, V., Schayes, G., Steeneveld, G. -J., Svensson, G. Taylor, P. A., Wunsch, S., Weng, W. and Xu, K.-M.: 2005, 'Single-Column Model Intercomparison for a Stably Stratified Atmospheric Boundary Layer', this issue .

Derbyshire, S. H.: 1990, 'Nieuwstadt's Stable Booundary Layer Revisited', *Quart. J. Roy. Meteorol. Soc.* **116**, 127–158 .

Delage, Y.: 1974, 'A Numerical Study of the Nocturnal Atmospheric Boundary Layer', *Quart. J. Roy. Meteorol. Soc.* **100**, 251–265.

Detering, H. W. and Etling, D.: 1985, 'Application of the E–ϵ Turbulence Model to the Atmospheric Boundary Layer', *Boundary-Layer Meteorol.* **33**, 113–133.

Freedman, F. R. and Jacobson, M. Z.: 2003, 'Modification of the Standard ϵ Equation for the Stable ABL through Enforced Consistency with Monin-Obukhov Similarity Theory', *Boundary-Layer Meteorol.* **106**, 384–410.

Garratt, J. R.: 1982, 'Observations in the Nocturnal Boundary Layer', *Boundary-Layer Meteorol.* **22**, 21–48.

Kantha, L. H. and Clayson, C. A.: 2000, '*Small Scale Processes in Geophysical Fluid Flow,*' Academic Press, San Diego, 888 pp.

Karpik, S. R.: 1988, 'An Improved Method for Integrating the Mixed Spectral Finite Difference (MSFD) Model Equations', *Boundary-Layer Meteorol.* **43**, 273–286.

Kosović, B. and Curry, J. A.: 2000, 'A Large-Eddy Simulation Study of a Quasi-Steady, Stably Stratified Atmospheric Boundary Layer', *J. Atmos. Sci.* **57**, 1052–1068.

Lenschow, D. H., Li, X. S., Zhu, C. J. and Stankov, B. B.: 1988, 'The Stably Stratified Boundary-Layer over the Great Plains: 1. Mean and Turbulence Structure', *Boundary-Layer Meteorol.* **42**, 95–121.

Mason, P. J. and King, J. C.: 1984, 'Atmospheric Flow over a Succesion of nearly Two-Dimensional Ridges and Valleys', *Quart. J. Roy. Meteorol. Soc.* **110**, 821–845.

Nieuwstadt, F. T. M.: 1984, 'The Turbulent Structure of the Stable, Nocturnal Boundary Layer', *J. Atmos. Sci.* **41**, 2202–2216.

Nieuwstadt, F. T. M.: 1985, 'A Model for the Stationary, Stable Boundary Layer', in J. C. R. Hunt (ed.), *Proceedings of the IMA Conference on Turbulence and Diffusion in the Stable Environment*. Cambridge, 1983, Clarendon Press, pp. 149–179.

Pasquill, F. and Smith, F. B.: 1983, *Atmospheric Diffusion*, Ellis Horwood, 3rd edn, 437 pp.

Weng, W. and Taylor, P. A.: 2003, 'On Modelling the One-Dimensional Atmospheric Bounday-Layer', *Boundary-Layer Meteorol.* **107**, 371–400.

Xu, D. and Taylor, P. A.: 1997, 'An E–ϵ–ℓ Turbulence Closure for Planetary Boundary-Layer Models: The Neutrally Stratified Case', *Boundary-Layer Meteorol.* **84**, 247–266.

Zilitinkevich, S. S.: 1972, 'On the Determination of the Height of the Ekman Boudnary Layer', *Boundary-Layer Meteorol.* **3**, 141–145.